Received: 5 May 2020 | Revised: 8 August 2020 | Accepted: 3 September 2020

DOI: 10.1002/jcc.26422

FULL PAPER

Journal of COMPUTATIONAL CHEMISTRY WILEY

A QM/MM simulation study of transamination reaction at the active site of aspartate aminotransferase: Free energy landscape and proton transfer pathways

Sindrila Dutta Banik | Arindam Bankura | Amalendu Chandra

Department of Chemistry, Indian Institute of Technology Kanpur, Kanpur, Uttar Pradesh, India

Correspondence
Amalendu Chandra, Department of Chemistry, Indian Institute of Technology Kanpur, Kanpur, UP 208016, India.
Email: amalen@iitk.ac.in

Present address
Sindrila Dutta Banik, Quantumzyme, Bengaluru, Karnataka, India

Arindam Bankura, Department of Chemistry, Midnapore College (Autonomous), Midnapore, West Bengal, India

Funding information
Science and Engineering Research Board (SERB); Council of Scientific and Industrial Research (CSIR), India

Abstract

Transaminase is a key enzyme for amino acid metabolism, which reversibly catalyzes the transamination reaction with the help of PLP (pyridoxal 5′-phosphate) as its cofactor. Here we have investigated the mechanism and free energy landscape of the transamination reaction involving the aspartate transaminase (AspTase) enzyme and aspartate-PLP (Asp-PLP) complex using QM/MM simulation and metadynamics methods. The reaction is found to follow a stepwise mechanism where the active site residue Lys258 acts as a base to shuttle a proton from α-carbon (CA) to imine carbon (C4A) of the PLP-Asp Schiff base. In the first step, the Lys258 abstracts the CA proton of the substrate leading to the formation of a carbanionic intermediate which is followed by the reprotonation of the Asp-PLP Schiff base at C4A atom by Lys258. It is found that the free energy barrier for the proton abstraction by Lys258 and that for the reprotonation are 17.85 and 3.57 kcal/mol, respectively. The carbanionic intermediate is 7.14 kcal/mol higher in energy than the reactant. Hence, the first step acts as the rate limiting step. The present calculations also show that the Lys258 residue undergoes a conformational change after the first step of transamination reaction and becomes proximal to C4A atom of the Asp-PLP Schiff base to favor the second step. The active site residues Tyr70* and Gly38 anchor the Lys258 in proper position and orientation during the first step of the reaction and stabilize the positive charge over Lys258 generated at the intermediate step.

KEYWORDS

aspartate transaminase enzyme, free energy landscape, proton transfer, pyridoxal 5′-phosphate, QM/MM metadynamics, transamination

1 | INTRODUCTION

Pyridoxal 5′-phosphate (PLP) is an ubiquitous cofactor which helps in catalyzing a variety of chemical transformations, such as racemization, decarboxylation, transamination, elimination, and substitution reactions.[1–4] The group of PLP dependent enzymes includes more than 145 distinct enzymes which constitute about 4% of the total cellular enzymes.[5–8] In addition to their versatility as catalysts, PLP dependent enzymes are also involved in widespread cellular processes such as the biosynthesis of amino acids and amino acid-derived metabolism. The role of these enzymes in many fundamental pathways makes them a potential target for drug designing. For example, serine hydroxyl methyl transferase (SHMT) has been identified as a target for cancer therapy,[9] *Plasmodium falciparum* aspartate transaminase is a potential drug target,[10] inhibitors of γ-aminobutyric acid aminotransferase (GABA Tase) are used in the treatment of epilepsy,[11] and inhibitors of ornithine decarboxylase (ODC) are employed in the treatment of African sleeping sickness.[12] Therefore,

it is important to investigate the function of these enzymes to understand their roles in medicinal and biological chemistry and also to develop new molecules capable of impairing enzymatic activity and to design improved protein based catalysts.[13]

The transaminase (Tase) is a PLP dependent enzyme which catalyzes the transamination reaction. According to the crystallographic studies,[5–8,14] the PLP initially forms a covalent bond with a conserved lysine residue of the transaminase enzyme which is usually referred to as the internal aldimine state. Subsequently, the PLP-enzyme complex reacts with the substrate amino acid where the bond between the active site lysine and PLP is broken and a new Schiff base is formed between the PLP and substrate amino acid which is referred to as the external aldimine state.[15] This step is commonly known as the transimination reaction which is the prerequisite for all PLP dependent enzymes.[16] After formation of the external aldimine, the PLP can catalyze a diverse variety of reactions as illustrated in Figure 1. The majority of the PLP catalyzed reactions are initiated by abstraction of α-proton of the substrate amino acid from the Schiff base compound by a Lys residue leading to the formation of a carbanionic intermediate.[17] The carbanionic intermediate is then stabilized via resonance and adopts the quinonoid geometry as shown in Figure 2. This carbanionic intermediate can undergo several different reactions. One of the most important reactions is the transamination reaction in which the intermediate undergoes reprotonation at the C4A atom of PLP resulting in the formation of ketimine. The ketimine on subsequent hydrolysis produces a keto acid. A schematic representation of the PLP-Asp Schiff base along with the numbering scheme of different atoms is shown in Figure 3. It may be noted that we have used the same numbering scheme as was followed in earlier work.[18]

The overall catalytic cycle of the transamination reaction can be divided into two halves as shown in Figure 4. In the first half of the reaction, an amino acid substrate is converted into its keto acid product, while in the second half of the reaction, another keto acid substrate is converted into its corresponding amino acid product.[19–22]The aspartate transaminase (AspTase) is one of the most extensively studied transaminase enzymes which catalyzes the reaction: L-aspartate +2-oxoglutarate ⇌ oxalacetate + L-glutamate. In apo-enzyme state (i.e., in absence of the PLP cofactor), the transaminase enzyme is catalytically inactive.[23–26] In the resting state of the catalytically active enzyme, the PLP has been found to be covalently linked to Lys258 (internal aldimine state).[5–8,14] This internal Schiff base is then converted into an external PLP-Asp Schiff base via displacement of Lys258 by the substrate Asp.[27–34] Subsequently, it has been suggested that the external aldimine undergoes a[1,3] proton transfer to form ketimine which, on hydrolysis, produces a keto acid. The mechanism of the[1,3] proton transfer process to produce ketimine from the external aldimine was proposed in earlier studies based on crystallography and kinetic isotope effects.[7,19,26,35–37] As per the proposed mechanism, the Lys258 residue of the enzyme abstracts the CA proton from PLP-Asp Schiff base yielding a carbanionic intermediate which gets stabilized via resonance and adopts the quinonoid structure. Formation of this quinonoid intermediate is then followed by reprotonation of the PLP-Asp complex at C4A atom which is generally known as the[1,3] proton transfer step. The reprotonation at C4A of the PLP-Asp Schiff base produces a ketimine. On hydrolysis, the ketimine yields a keto acid and PMP. Then, the second keto acid reacts with PMP to form the corresponding chiral amino acid and thereby regenerates the PLP. Finally, Lys258 reconnects to the cofactor PLP by displacing the amino acid. Figure 4 shows this suggested reaction scheme of the transamination reaction. If no keto acid is present, only the first half of transamination reaction can occur.[23]

As described above, it is generally believed that the[1,3] proton transfer process involves a quinonoid intermediate for the proton shift from CA to C4A.[7,19,26,35–37] However, the details of the reaction mechanism and the free energetics of the proton transfer process are still not fully understood. For example, very little is known at the moment regarding the free energy landscape, reaction barriers and proton transfer pathways on the free energy landscape for the formation of quinonoid intermediate and then the ketimine product. Also, it may be noted that a concerted single step mechanism has been proposed for cytoplasmic isozyme AATase with L-aspartate while a stepwise mechanism has been suggested for mitochondrial AATase with L-glutamate.[38] The deuterium isotope effects show that the abstraction of the CA proton, ketimine hydrolysis and oxaloacetate dissociation is the rate limiting step.[39] Kinetic studies suggested that the[1,3] proton transfer is the rate determining step.[40,41] The reaction mechanism of the second half of the transamination reaction (ketimine → aldimine) in a small model of the active site of AspTase has also been studied using computational method. The results show that the proton abstraction from the C4A atom by Lys258 is the rate limiting step.[42] However, to the best of our knowledge, the details of the reaction mechanism of the first half of the transamination reaction including the free energy barriers and proton transfer pathways on the free energy landscape have not been studied yet. Such studies are essential for having a better understanding and more complete

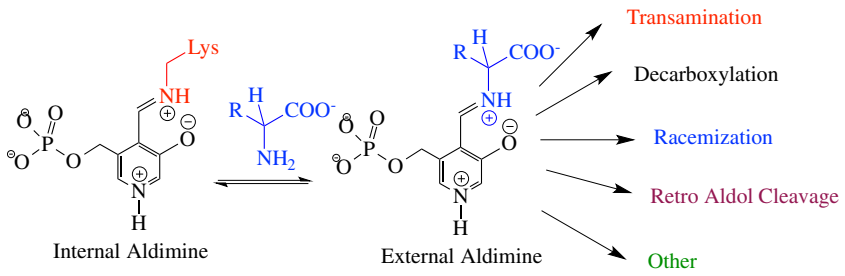

FIGURE 1 Reaction scheme of the common step of PLP dependent enzymes which is followed by different reactions for different enzymes. Several other reaction types are not shown explicitly for clarity [Color figure can be viewed at wileyonlinelibrary.com]

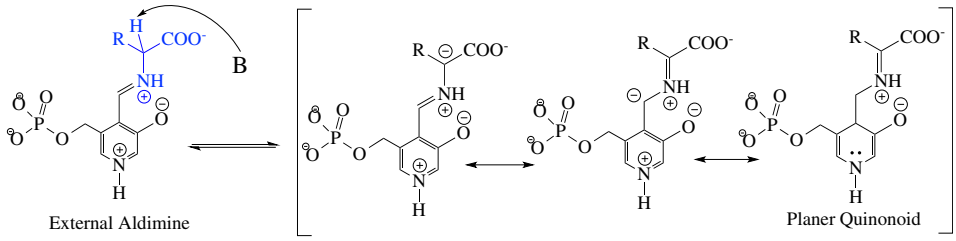

FIGURE 2 Resonance structures of the carbanionic intermediate. The quinonoid structure is shown on the right [Color figure can be viewed at wileyonlinelibrary.com]

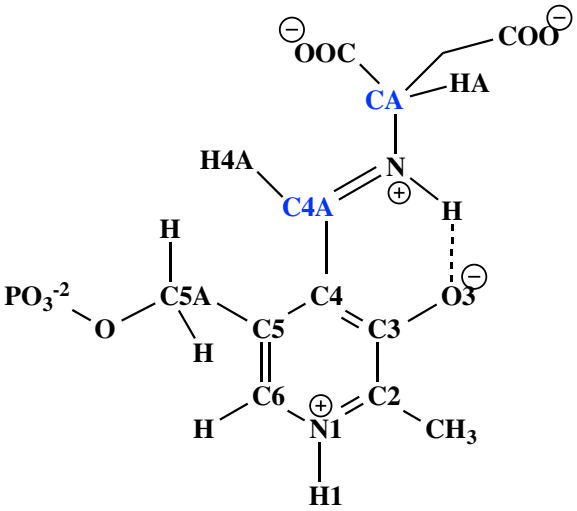

FIGURE 3 Schematic representation of the PLP-Asp Schiff base with the atom numbering scheme. The carbon atoms which act as proton abstraction (CA) and reprotonation sites (C4A) are shown in blue color [Color figure can be viewed at wileyonlinelibrary.com]

description of biological reactions.[43] In particular, it is important to perform such studies by considering the full protein, cofactor and substrate in explicit aqueous medium. The present work makes a contribution toward this end.

In the present work, we have studied the reaction mechanism of the formation of ketimine from the external aldimine state that involves the[1,3] proton transfer process at the active site of AspTase. As discussed above, this is an important step of the amino acid metabolism process. We note that the proton transfer at the active site of the enzyme involves bond breaking and formation and changes in polarization of the charge density. Thus, simulations of such reactions require suitable quantum mechanical treatment of the active site of the enzyme. Here we have employed the method of quantum-classical (QM/MM) molecular dynamics (MD) where the technique of ab initio MD is combined with empirical force field based simulations. We note that the method of QM/MM calculations have been used rather extensively to study the mechanism and energetics of many enzymatic reactions in the past.[44–53] However, to the best of our knowledge, such a study of the mechanism and free energies of transamination reaction considering full structural details of the enzyme, PLP, substrate and the surrounding environment is presented here for the first time. Specifically, we have used the Car–Parrinello method[54] for ab initio MD and AMBER[55] force fields for the classical MD to perform QM/MM[44,45] simulations of the transamination reaction at active site of the aspartate transaminase enzyme. Further, we employed the metadynamics method,[56,57] to study the reaction pathways connecting various states and obtain the associated structures, free energy barriers of their interconversions and also the overall free energy landscape in the multi-dimensional collective variable (CV) space.

The rest of the article is organized as follows. The details of the calculations are described in Section 2. The results are discussed in Section 3 and our conclusions are summarized in Section 4.

2 | DETAILS OF SIMULATIONS

The homodimeric crystal structure of cytoplasmic AspTase (1ARG.pdb)[58] from *Escherichia coli* complexed with PPD (pyridoxyl-aspartic acid 5′ monophosphate) has been used for the present calculations. Each subunit is comprised of two domains and there are two active sites and two PLPs per dimer. The two active sites are located at interface of the two subunits. Each PLP is positioned at the bottom of the active site pocket and the residues create a network of interaction with the PLP-Asp Schiff base. This is shown in Figure 5. The substrate (i.e., the PLP-Asp Schiff base) was generated by modifying the structure of PPD. Our earlier study has shown that the keto form of PLP Schiff base is more preferred at the active site of AspTase.[18] Hence, in the current work, we have looked at the transamination reaction for the N-protonated tautomer of the PLP Schiff base. The protonation states of the active site residues were considered to be the same as described in our earlier work.[18]

The substrate was modeled by using the generalized amber force field (GAFF)[59] together with the RESP point charges computed using RED package.[60] The amber force field (leaprc.ff99SB) was used for the protein.[55] The dimeric protein was solvated in a rectangular box of dimension 112 Å × 119 Å × 91 Å containing 29,833 TIP3P[61] water molecules as solvent and also 500 crystallographic water molecules which were embedded in the protein. The system was neutralized by adding $22Na^+$ ions. Altogether, the simulation system contained 1,03,271 atoms. The classical MD simulation was performed by following the same protocols as described in earlier work.[18] The classically equilibrated system was subjected to re-equilibration in hybrid QM/MM framework[44,45] where the system was partitioned into its quantum and classical parts. All the atoms of the substrate PLP-Asp Schiff base and the side chain of Lys258 were treated quantum mechanically which contained 52 atoms. The QM

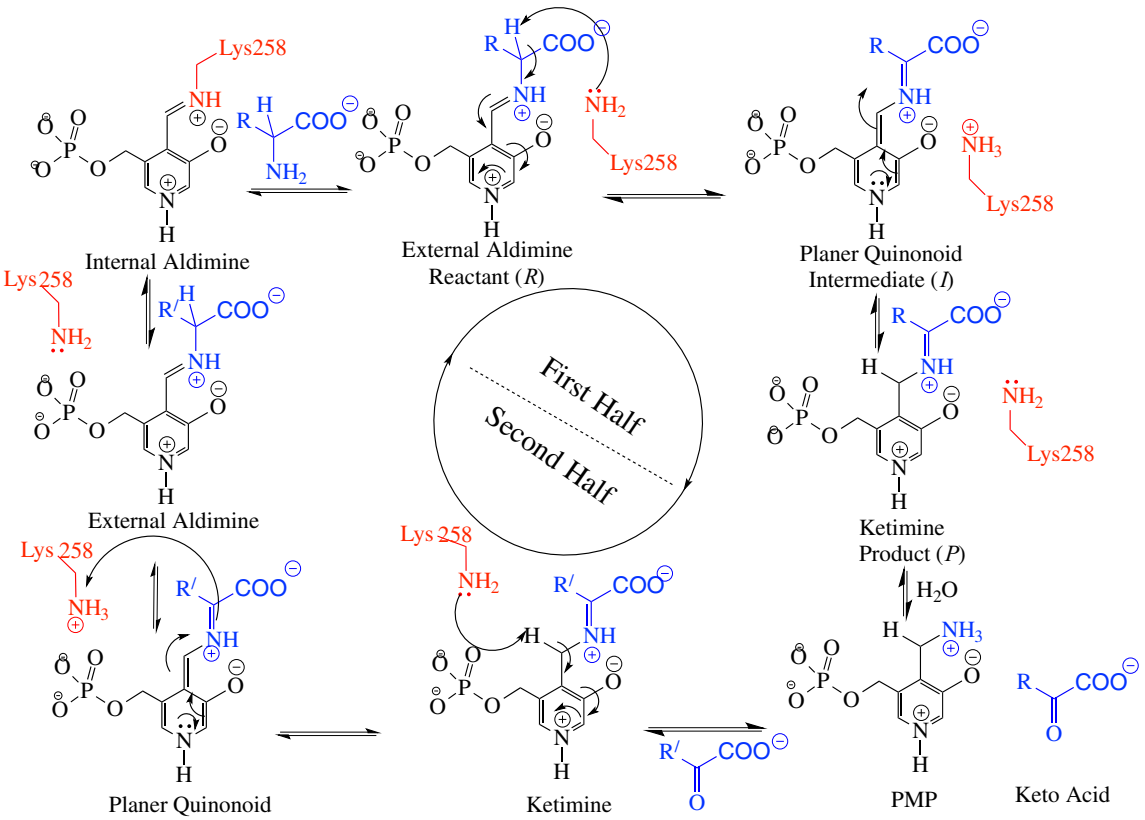

FIGURE 4 Schematic representation of the reaction mechanism of the transamination reaction at the active site of AspTase. This scheme was suggested based on the crystallographic study as well as studies based on kinetic isotope effects[7,19,26,35–37] [Color figure can be viewed at wileyonlinelibrary.com]

supercell used in the present case had the dimension of 22 Å × 22 Å × 22 Å. The QM/MM boundary was set between $C_\alpha - C_\beta$ bond. The dangling bond of C_β atom in QM part was saturated by capping a hydrogen atom. We used the interface of CPMD/GROMOS96[62] for the current QM/MM simulations.

We employed the BLYP exchange-correlation functional[63,64] in the present calculations. The core electrons of all the atoms were treated by Troullier–Martins norm-conserving pseudopotentials[65] and the plane wave expansion of the valence-electron wave function was truncated at a kinetic energy cut-off of 70 Ry. All hydrogen atoms were given the mass of deuterium which allows a slightly longer time step. The simulations were carried out with a time step of 4 au and a fictitious electronic orbital mass of 400 au. Before metadynamics simulation, we re-equilibrated the classically equilibrated system for about 10 ps through QM/MM simulation in the NVT ensemble at 300 K using the Nose–Hoover chain thermostat.

Metadynamics is a MD based technique in which sampling is facilitated by the introduction of an additional bias potential that acts on selected degrees of freedom that are relevant for the chemical reaction of interest. These degrees of freedom are referred to as the CVs.[56,57,66–68] A CV S_α(R) is a function of the Cartesian coordinates R of the nuclei which differentiates the reactant and product states and describes the slowest modes in the process of interest. In the extended Lagrangian formulation of metadynamics that has been used here, a set of auxiliary degrees of freedom s_α (called auxiliary or fictitious variables) with velocity $\dot{s}_\alpha$, mass μ_α, equal in number to chosen CVs are introduced to the standard Lagrangian $\mathscr{L}_{CP}$ to continuously explore the space of CVs. Starting from the Car–Parrinello Lagrangian,[54] the form of the extended Lagrangian for the metadynamics is expressed as follows.[56,57]

$$\mathscr{L}^{MTD} = \mathscr{L}_{CP} + \sum_{\alpha=1}^{N_s} \frac{1}{2}\mu_\alpha^s \dot{s}_\alpha^2(t) - \sum_{\alpha=1}^{N_s} \frac{1}{2} k_\alpha [S_\alpha(R(t)) - s_\alpha(t)]^2 + V(t,[s]) \,, \quad (1)$$

where, the first term is the standard Car–Parrinello Lagrangian, the second term is the fictitious kinetic energy associated with the fictitious variable s_α, the third term is a harmonic potential with force constant k_α that restrains the value of the instantaneous CVs S close to the corresponding dynamic auxiliary variables s and the fourth term is a history dependent repulsive bias potential which is a functional of the entire path [s].

In the present work, $V(t,[s])$ is chosen to be a Gaussian potential with width and height of 0.04 au and 0.0008 au, respectively. We have chosen two CVs, defined in terms of coordination number differences (ΔN_{coord}), to simulate the transformation from α-amino acid → α-keto acid in the present calculations. The coordination number difference is defined as follows.[57,69,70]

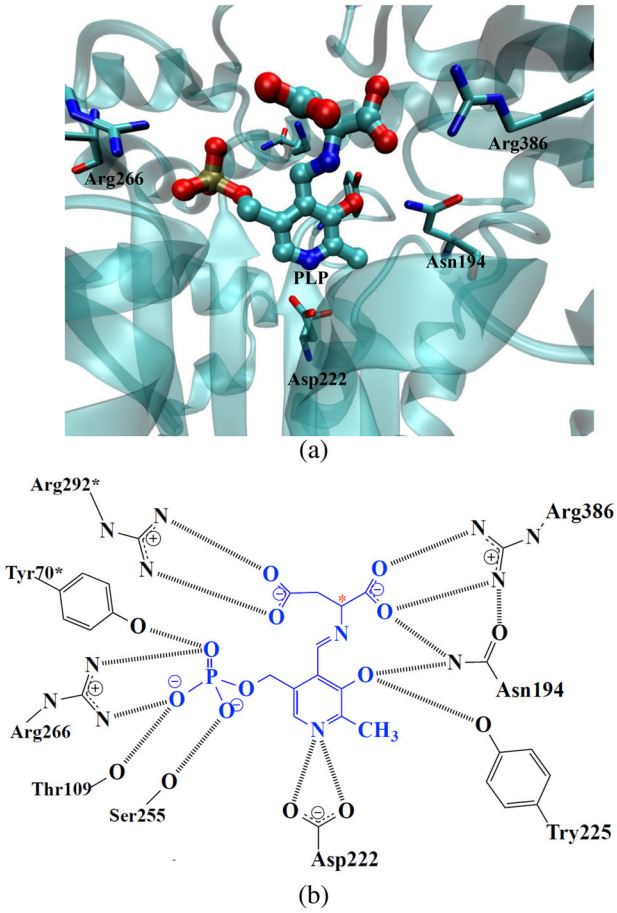

FIGURE 5 (a) Structure of the active site of Aspartate transaminase (AspTase) complexed with pyridoxyl-aspartic acid 5′ monophosphate (PDB code: 1ARG).[58] The structure is the basis of the model used in the present work. The reactants (PLP-Asp Schiff base) are shown in CPK style. Side chains of the active site residues in close proximity of the reactants such as Asn194, Asp222, Tyr225, Lys258, Arg266, and Arg386 are shown by bonds. The image is prepared using VMD.[78] (b) Schematic representation of the hydrogen bonding interactions between the PLP-Asp complex and the active side residues. The PLP-Asp Schiff base is shown using blue color [Color figure can be viewed at wileyonlinelibrary.com]

$$\Delta N_{\text{coord}}(A,B;C) = N_{\text{coord}}(AC) - N_{\text{coord}}(BC) = \left[\frac{1-(r_{AC}/d_{\text{cut}})^{p}}{1-(r_{AC}/d_{\text{cut}})^{(p+q)}}\right] - \left[\frac{1-(r_{BC}/d_{\text{cut}})^{p}}{1-(r_{BC}/d_{\text{cut}})^{(p+q)}}\right] \quad (2)$$

where r_{AC} and r_{BC} are the interatomic distances, d_{cut} is a threshold distance for bonding and p and q are exponents which determine the steepness of the decay of ΔN_{coord} with respect to r_{AC} and r_{BC}. The coupling constant k_α and mass μ_α depend on the type of CVs used and are chosen to be 2.0 au and 20 amu, respectively, for both CVs considered here.

In the present work, two CVs, CV1 and CV2, are considered to study the multi-step proton transfer process associated with the conversion of α-amino acid to α-keto acid by means of metadynamics simulations. The difference between the coordination number of $Lys_{258}N_\zeta$ and CA atom of Asp-PLP Schiff base with respect to the hydrogen atoms ($Lys_{258}H_\zeta$ and HA) is taken as CV1. This is a measure of the degree of proton transfer from the α carbon atom of the PLP molecule (CA) to N_ζ atom of Lys258 ($Lys_{258}N_\zeta$). The CV1 can be represented as Δ N_{coord} ($Lys_{258}N_\zeta$, CA; $Lys_{258}H_\zeta$, HA) = N_{coord} ($Lys_{258}N_\zeta$; $Lys_{258}H_\zeta$, HA) $-N_{\text{coord}}$(CA; $Lys_{258}H_\zeta$, HA). Similarly, the coordination number difference between the $Lys_{258}N_\zeta$ and C4A carbon atom of Asp-PLP Schiff base with respect to the hydrogen atoms ($Lys_{258}H_\zeta$, H4A) are considered as CV2. The CV2 can be represented as ΔN_{coord} ($Lys_{258}N_\zeta$, C4A; $Lys_{258}H_\zeta$, H4A) = N_{coord} ($Lys_{258}N_\zeta$; $Lys_{258}H_\zeta$, H4A) $-N_{\text{coord}}$ (C4A; $Lys_{258}H_\zeta$, H4A).The use of coordination number difference as a CV imposes flexibility in the model. A simple CV like distance would bias a particular hydrogen atom of Lys258 to be transferred to C4A during the simulation. While, the coordination number difference allows any of the hydrogen atoms of the amino group of Lys258 to coordinate with the C4A atom of the PLP-Asp Schiff base.

In order to understand the free energy surface involving these generalized coordinates, first we need to have a look at how the CVs will change along the reaction path. At the beginning of the simulation, one hydrogen atom is coordinated with the CA atom of PLP (via CA–HA bond) [N_{coord}(CA; $Lys_{258}H_\zeta$, HA) = 1] and two hydrogen atoms are coordinated with $Lys_{258}N_\zeta$ ($Lys_{258}N_\zeta$-$Lys_{258}H_\zeta$) [N_{coord}($Lys_{258}N_\zeta$; $Lys_{258}H_\zeta$, HA) = 2], thus CV1 = ΔN_{coord} ($Lys_{258}N_\zeta$, CA; $Lys_{258}H_\zeta$, HA) ≈1.0 in the reactant state. In the intermediate state, no hydrogen atom is bonded to CA [N_{coord} (CA; $Lys_{258}H_\zeta$, HA) = 0] and three hydrogen atoms are bonded to $Lys_{258}N_\zeta$ ($Lys_{258}N_\zeta$-$Lys_{258}H_\zeta$) [N_{coord} ($Lys_{258}N_\zeta$; $Lys_{258}H_\zeta$, HA) = 3], thus CV1 = ΔN_{coord} ($Lys_{258}N_\zeta$, CA; $Lys_{258}H_\zeta$, HA) ≈3.0. At the end of the reaction, no hydrogen atom is bonded to CA [N_{coord} (CA; $Lys_{258}H_\zeta$, HA) = 0] and two hydrogen atoms are bonded to $Lys_{258}N_\zeta$ ($Lys_{258}N_\zeta$-Lys_{258} H_ζ) [N_{coord} ($Lys_{258}N_\zeta$; $Lys_{258}H_\zeta$, HA) = 2], thus CV1 = ΔN_{coord} ($Lys_{258}N_\zeta$, CA; $Lys_{258}H_\zeta$, HA) ≈2.0. On the other hand, at the beginning of the simulation, one hydrogen atom is coordinated with the C4A atom of PLP (C4A-H4A) [N_{coord} (C4A; $Lys_{258}H_\zeta$, H4A) = 1] and two hydrogen atoms are coordinated with $Lys_{258}N_\zeta$ (Lys_{258} N_ζ-$Lys_{258}H_\zeta$) [N_{coord} ($Lys_{258}N_\zeta$; $Lys_{258}H_\zeta$, H4A) = 2], thus CV2 = ΔN_{coord} ($Lys_{258}N_\zeta$, C4A; $Lys_{258}H_\zeta$, H4A) ≈1.0 in the reactant state. In the intermediate state, one hydrogen atom is bonded to C4A [N_{coord} (C4A; $Lys_{258}H_\zeta$, H4A) = 1] and three hydrogen atoms are bonded to $Lys_{258}N_\zeta$ ($Lys_{258}N_\zeta$-$Lys_{258}H_\zeta$) [N_{coord} ($Lys_{258}N_\zeta$; $Lys_{258}H_\zeta$, H4A) = 3], thus CV2 = ΔN_{coord} ($Lys_{258}N_\zeta$, C4A; $Lys_{258}H_\zeta$, H4A) ≈2.0. At the end of the reaction, two hydrogen atoms are bonded to C4A [N_{coord} (C4A; Lys_{258} H_ζ, H4A) = 2] and two hydrogen atoms are bonded to $Lys_{258}N_\zeta$ ($Lys_{258}N_\zeta$-$Lys_{258}H_\zeta$) [N_{coord} ($Lys_{258}N_\zeta$; $Lys_{258}H_\zeta$, H4A) = 2], thus CV2 = ΔN_{coord} ($Lys_{258}N_\zeta$, C4A; $Lys_{258}H_\zeta$, H4A) ≈0.0. Therefore, the values of the CVs at the initial state (CV1, CV2 ≈ 1.0, 1.0) and final state (CV1, CV2 ≈ 2.0, 0.0) are different enough to ensure that the two states will appear in different region of the free energy surface which is a necessary condition for a suitable characterization of the reaction path in a metadynamics simulation. The values of the CVs corresponding to the reactant, intermediate and product states are included in Table 1. As discussed above, the current CVs in terms of differences in coordination numbers naturally

TABLE 1 Values of the collective variables in the reactant, intermediate and product states

Collective variable	Reactant	Intermediate	Product
CV1	1	3	2
CV2	1	2	0

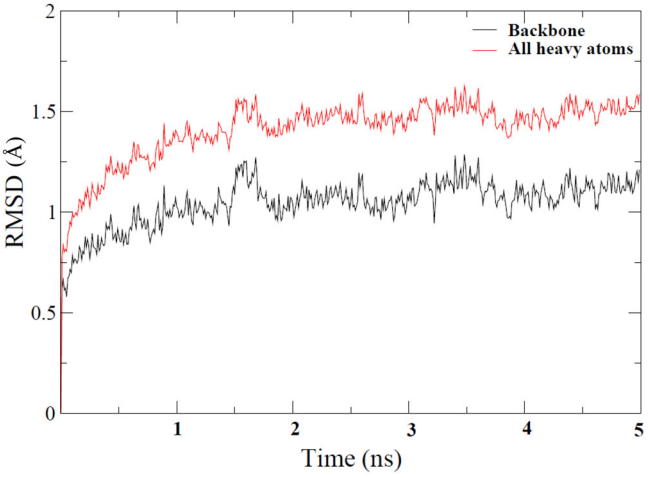

FIGURE 6 The root mean square deviation (RMSD) of the protein backbone as well as all heavy atoms with respect to the starting structure of the NVT simulation during the empirical force field based MD simulation for AspTase [Color figure can be viewed at wileyonlinelibrary.com]

capture the progress of the reaction from reactant to product through the intermediate state (Table 1). These CVs constitute the reaction coordinate space where the chemical process of interest can be clearly described through different locations of the reactant, intermediate and the product states. Such CVs involving coordination numbers have also been successfully used earlier for exploring biochemical reactions.[50,51,53]

3 | RESULTS AND DISCUSSION

3.1 | Solvated structure and interactions

At first, we discuss the results of classical simulation that was performed for the solvated AspTase along with PLP-Asp Schiff base. The root mean square deviation (RMSD) of the protein backbone is found to be less than 2 Å with respect to the first frame of the NVT simulation which reflects that the protein structure was stable throughout the simulation. This is shown in Figure 6. The variation in the separation between donor CA atom of PLP-Asp Schiff base and acceptor $Lys_{258}N_{\zeta}$ atom and also the separation between HA atom (which would be transferred in the first step of transamination reaction) of PLP and acceptor $Lys_{258}N_{\zeta}$ atom are shown in Figure 7 for both the chains. The results show that the separations

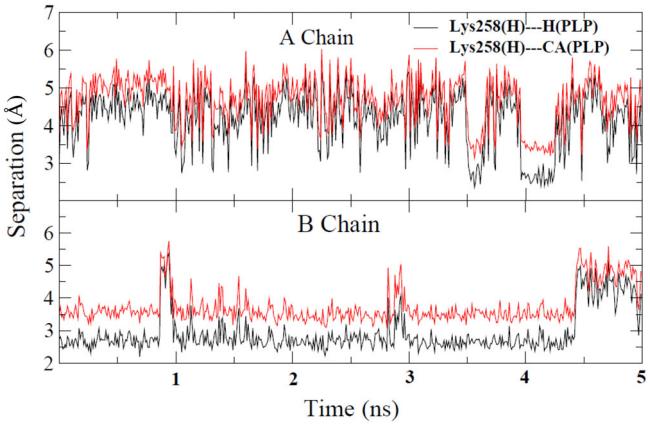

FIGURE 7 Variation in the separation between $Lys_{258}N_{\zeta}$ and HA atom of PLP (in black) and separation between $Lys_{258}N_{\zeta}$ and CA atom of PLP (in red) during the empirical force field based MD simulation for (a) A chain, and (b) B chain of the AspTase enzyme [Color figure can be viewed at wileyonlinelibrary.com]

vary randomly at individual active sites. Since the donor-acceptor distances can be directly linked to favorable reactive conformations, it may be concluded that the appearances of reactive conformations of chains A and B are not synchronized, rather they take place in an independent manner. This also implies that the reaction occurs in the two chains independently. The experimental results also show independent catalytic function of the two active sites of the AspTase dimer.[71] The average CA....$Lys_{258}N_{\zeta}$ separation is found to be 4.68 and 4.16 Å for chains A and B, respectively. The corresponding HA....$Lys_{258}N_{\zeta}$ separation is found to be 3.73 and 2.93 Å on average for the A and B chains. Figure 7 shows that the favorable configuration of Lys258 for proton transfer or the reactive conformation is rather short lived for chain A, whereas the reactive conformation is found to be longer lived for chain B in the current simulation. As the number of reactive conformations is more for chain B, one such favorable reactive conformation is selected from chain B, and is used for modeling of the reaction in subsequent calculations.

The present MD simulations also show that the PLP-Asp Schiff base is embedded in a network of hydrogen bonding interactions at the active site of AspTase. The protonated pyridine nitrogen (N1) of PLP strongly interacts with Asp222. A protonated pyridine ring has been proposed to serve as an electron sink to stabilize the carbanionic intermediate produced during the reaction[42] and is critical for catalysis. The indole ring of Trp140 is stacked over the pyridine ring of PLP. Both Arg292* (* indicates residue from the second subunit) and Arg386 form strong hydrogen bonds with β and α carboxylate groups of the substrate, respectively. The Asn194 is found to be involved in multiple hydrogen bonding interactions with PLP-Asp Schiff base including the phenolic oxygen (O3) of PLP and carboxylate group of the substrate. The phosphate moiety of PLP contains two negative charges and interacts with the positively charged Arg266. It also forms hydrogen bonds with hydrogen bond donors such as peptide backbone of Gly108 and the side chains of Thr109, Ser255, Tyr70*.

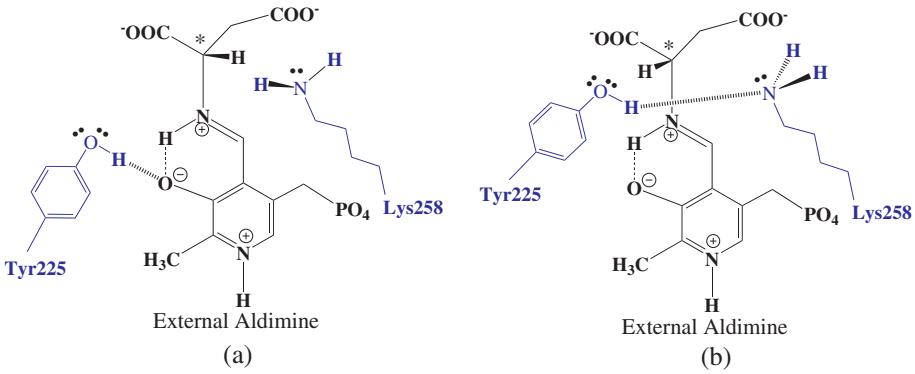

FIGURE 8 Schematic representation of the hydrogen bonding interactions of Tyr225 with PLP and Lys258 in different time intervals. (a) Tyr225 acts as hydrogen bond donor to the O3 atom of PLP; (b) Tyr225 acts as hydrogen bond donor to the N atom of Lys258 [Color figure can be viewed at wileyonlinelibrary.com]

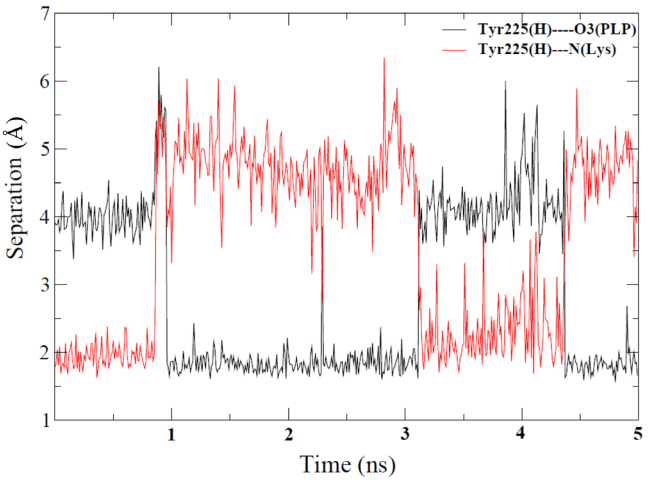

FIGURE 9 Changes in separation between the Tyr_{225}(H) and the O3 atom of PLP (in black) and that between the Tyr_{225}(H) and the $Lys_{258}N_{\zeta}$ atom of Lys258 (in red) for the B chain of AspTase enzyme during the force field based simulation [Color figure can be viewed at wileyonlinelibrary.com]

All these interactions are found to be stable throughout the simulation period.

Interestingly, the present MD simulation results show two different hydrogen-bonding pattern for the Tyr225. This is shown in Figure 8. In the first case (Figure 8a), Tyr225 acts as hydrogen bond donor to the O3 atom of PLP and the $Lys_{258}N_{\zeta}$ lone pair is positioned in a suitable orientation to interact with the HA atom of PLP. This hydrogen bonding pattern suggests a direct proton transfer from CA to $Lys_{258}N_{\zeta}$. While, in the second case, the Tyr225 acts as a hydrogen bond donor to the $Lys_{258}N_{\zeta}$ and one $Tyr_{225}O_{\eta}$ lone pair is positioned in a suitable orientation to interact with the HA of PLP as shown in Figure 8b. This hydrogen bonding pattern suggests indirect proton transfer via the Tyr225. First the proton will have to be transferred from CA to $Tyr_{225}O_{\eta}$ and then from $Tyr_{225}O_{\eta}$ to $Lys_{258}N_{\zeta}$. The changes in the separation between $Tyr_{225}O_{\eta}$ and O3 atom of PLP and that between $Tyr_{225}O_{\eta}$ and $Lys_{258}N_{\zeta}$ corresponding to two different hydrogen bonding patterns are shown in Figure 9. The results show that the second configuration, where the $Tyr_{225}O_{\eta}$ interacts with $Lys_{258}N_{\zeta}$ through a hydrogen bond, is relatively short lived than the first configuration. The average $Tyr_{225}O_{\eta}$...HA separation is found to be greater than the $Lys_{258}N_{\zeta}$...HA separation, which seems to suggest that the direct pathway is more favorable than the indirect one. In the crystal structure, the static $Tyr_{225}O_{\eta}$...CA separation is 3.91 and 4.10 Å in the A and B chains, respectively. The $Lys_{258}N_{\zeta}$...CA separation is 3.51 and 3.53 Å, respectively, for the A and B chains. Thus, from the experimental crystal structures also, the probability of the indirect pathway is judged to be less than the direct path for the first step of the[1,3] proton transfer process, Consequently, we have studied the reaction mechanism of the[1,3] proton transfer process considering the direct pathway only. We also note in this context that a recent computational study using a small model of the active site also proposed that the proton transfer can take place by two different pathways: directly or with the assistance of a water molecule. However, no significant difference in the energy profiles was observed for the two pathways.[17] In the current study which used a full model of the enzyme including its active sites, no water was found to be present in the vicinity of the reactants at the active site, hence no water mediated proton transfer was considered.

3.2 | Free energy landscape and proton transfer pathways

The AspTase catalytic cycle involves two proton transfer reactions in each half-cycle. In the α-amino acid $\rightarrow$ α-keto acid half-cycle, the Lys258 abstracts the CA proton from PLP-Asp Schiff base to yield a carbanion intermediate, which is followed by the transfer of another proton from Lys258 to C4A atom of the PLP-Asp Schiff base. Here we have studied the structural and free energy details of the above proton transfer pathways by using the QM/MM metadynamics method. The coordination number can be used as a convenient variable to detect the presence of bond between two atoms or for counting the number bonds between two different atomic species. In the present work, we have chosen two CVs (CV1 and CV2) defined in terms of the coordination number differences (ΔN_{coord}) as described in Section 2 to carry out metadynamics simulation of the first half-cycle of the transamination reaction starting from the external

aldemine structure of the PLP-Asp Schiff base at the active site of the AspTase enzyme.

The free energy surface constructed from the metadynamics simulation is shown in Figure 10. The energy surface demonstrates that the transamination reaction proceeds via a stepwise mechanism as evidenced by the presence of a stable Asp-PLP carbanion intermediate. The contour plots shown at the base of Figure 10 also show that the path connecting the reactant (R) and product (P) minima through the intermediate (I) is of lower energy compared to any other direct path from R to P that bypasses the intermediate. The direct pathway from R to P (without passing through I) would involve a higher free energy barrier, which confirms the stepwise mechanism for the reaction under study. The free energy surface also shows that the proton transfer from the CA atom of Asp-PLP Schiff base to Lys258 is the rate limiting step for the[1,3] proton transfer process. The rate limiting step of the abstraction of CA proton by Lys258 is followed by the reprotonation of C4A atom by Lys258.The calculated free energy barrier for the proton abstraction by Lys258 is found to be 17.85 kcal/mol, which is comparable with the experimental value of around 14–16 kcal/mol extracted using classical transition state theory[42] from experimental rate constants for transamination in AATase from different organisms with oxoglutarate.[72–74] We also note that a recent computational study reported a barrier of around 19.3 kcal/mol for the reaction for a small model of the active site of the transaminase enzyme.[17]The agreement between the results of the present work and earlier estimate from experimental rate constants is rather good considering the computational complexity involved in modeling the enzymatic process. It is found from the metadynamics trajectory that the proton shuttling continued between the CA atom of Asp-PLP Schiff base and $Lys_{258}N_{\zeta}$ until the separation between these two atoms increased sufficiently. A complete transfer of proton and subsequent increase in the separation resulted in the formation of the intermediate. The corresponding snapshots of the structures of the reactant state, transition state-I, intermediate, transition state-II and the product state are shown in Figure 11a–e.

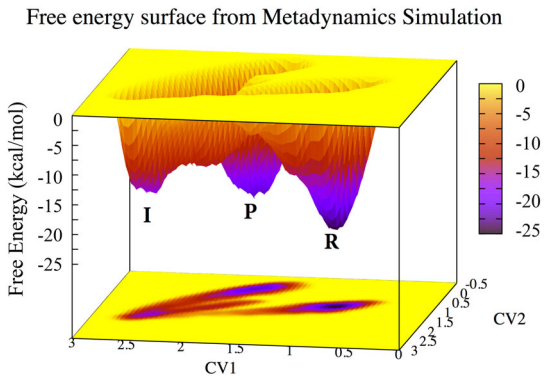

FIGURE 10 The calculated free energy surface for the transamination reaction. The free energies are expressed in kcal/mol. The R, I, and P represent the reactant, intermediate, and product, respectively. See Figure 11 for the structures of R, I, and P, and also the transition states for R → I and I → P reactions [Color figure can be viewed at wileyonlinelibrary.com]

Figure 10 also shows that the intermediate is 7.14 kcal/mol higher in energy than the external aldimine. In the intermediate state, the internal torsion about the dihedral angle of N-C4A-C4-C3 is restricted which implies a coplanar geometry with the pyridine ring. The restricted dihedral angle also implies that a strong intramolecular hydrogen bond exists between hydrogen and either imine nitrogen (N) or phenolic oxygen (O3) of PLP. The planar geometry of the intermediate state signifies that the negative charge over the CA atom is first stabilized by the neighboring protonated imine nitrogen (N) via electrostatic interaction and further delocalized into the protonated pyridine ring of PLP, which acts as an electron sink, to form a quinonoid intermediate. It is found from the metadynamics simulation that the CA….N separation decreases as well as the bond angles associated with the CA atom increase on going from reactant to the intermediate state. The changes in the bond angles and bond distances are likely caused by a rehybridization at the CA position from sp^3 to sp^2 along the transamination reaction pathway. Additionally, the decrease in the C4A….C4 separation indicates that a double bond character is developed between the C4A and C4 atom in the intermediate state which confirms the quinonoid geometry of the Asp-PLP Schiff base shown in Figure 2.

The free energy barrier for the reprotonation of PLP-Asp Schiff base at the C4A site from Lys258 is found to be 3.57 kcal/mol which is comparable with the value of around 4 kcal/mol reported in a recent computational study which used a small model of the active site of the transaminase enzyme.[17]The metadynamics trajectory shows that, in the transition state, the proton is delocalized between the $Lys_{258}N_{\zeta}$ and C4A atoms of the PLP-Asp Schiff base. The coplanarity of the Asp-PLP Schiff base is lost in the product state. The bond angles associated with the C4A atom decrease and the C4A….C4 and C4A…N separations increase relative to the reactant and intermediate states. The variation in the geometry of the Schiff base shows that the addition of the proton at C4A atom changes its configuration from the planer state to a tetrahedral state, thus the C4A atom is rehybridized from sp^2 to sp^3.

A look into the hydrogen bonding pattern at the active site of AspTase, shown in Figure 11, reveals that the active site residues play an important role during the reaction. The positive charge generated over the Lys258 residue during the first step of the reaction is stabilized by the surrounding active site residues such as Tyr70* and Gly38. The phenolic oxygen of Tyr70* side chain and the peptide backbone of Gly38 interact with the amino group of Lys258 as a hydrogen bond acceptor. These interactions provide suitable positioning and orientation of the Lys258 for proper catalytic activity. Additionally, the Tyr70* and the peptide backbone of Gly38 interact with the PLP-Asp Schiff base. The Tyr70* acts as hydrogen bond donor to the phosphate group of PLP and the peptide backbone of Gly38 interacts with the α-carboxylic acid group of the substrate. Consequently, these two residues anchor both the substrate and Lys258 and play an important catalytic role in the reaction pathway. We note in this context that a recent study also showed that the active site residues

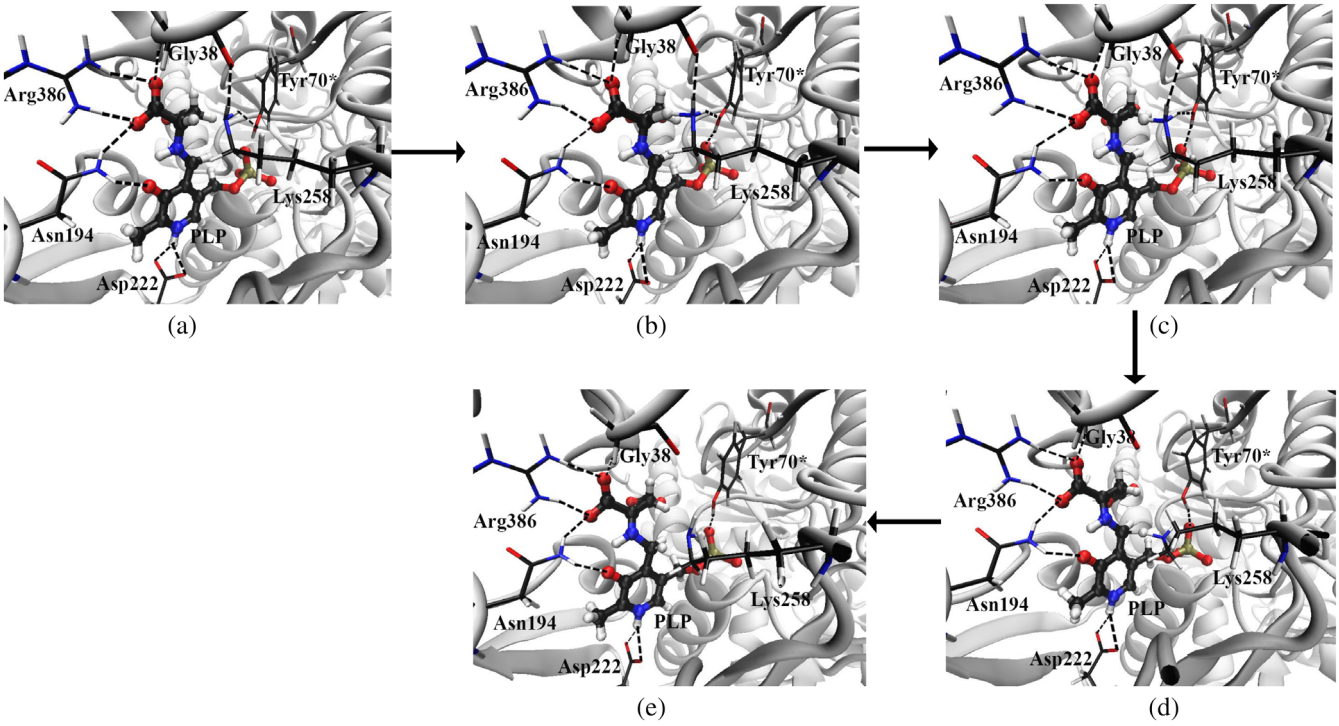

FIGURE 11 Snapshots of the (a) reactant, (b) transition state-1, (c) Intermediate, (d) transition state-2, and (e) product for the transamination reaction observed during the metadynamics simulation. The images are prepared using VMD[78] [Color figure can be viewed at wileyonlinelibrary.com]

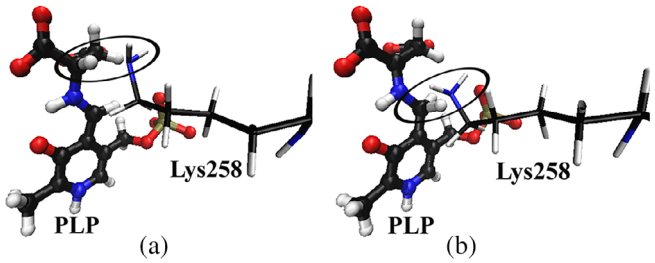

FIGURE 12 Snapshots of the active site pocket of AspTase showing the relative orientation of Lys258 with respect to the PLP Schiff base. (a) The amino group of Lys258 is in close proximity to the CA atom of PLP Schiff base, (b) The amino group of Lys258 is in close proximity to the C4A atom of the PLP Schiff base [Color figure can be viewed at wileyonlinelibrary.com]

create a network of interactions which favor the enzymatic reaction.[75] The current study also reveals similar supportive interactions from the active site residues to favor the enzymatic process of transamination reaction.

An analysis of Mulliken charges along the reaction path shows that the negative charge population on the pyridine nitrogen (N1) increases on going from the reactant state to the intermediate state and again decreases from the intermediate state to the product state. This confirms that the negative charge over the CA atom is delocalized over the pyridine ring of PLP in the intermediate state. The positive charge over the amino group of Lys258 increases along the first step and decreases in the second step. It is found form the metadynamics simulation that the Lys258 undergoes a conformational change during the[1,3] proton transfer process. This is shown in Figure 12. The major difference between the two conformations shown in Figure 12 is the relative orientation of the amino group of Lys258 with respect to the PLP-Asp Schiff base. In the first conformation, the amino group of Lys258 maintains its close proximity to the CA atom of PLP so that it can abstract the α-proton. After the proton abstraction, it undergoes a conformational change and becomes proximal to the C4A atom of PLP. In this configuration, the reprotonation of the PLP-Asp Schiff base through proton transfer from Lys258 to the C4A atom of PLP takes place. This conformational change of Lys258 is believed to be an essential feature for occurrence of the transamination reaction.

It is well known that the PLP-Asp complex undergoes an intramolecular proton transfer between the N-protonated and O-protonated tautomers. An earlier computational study showed that at the active site of Dopa decarboxylase, the O-protonated configuration is preferred both in the Michaelis complex and decarboxylation transition state.[76,77] However, a recent study based on QM/MM metadynamics simulations found that the N-protonated state of the PLP-Asp Schiff base is more suitable than the O-protonated one at the active site of AspTase.[18] Therefore, in the present calculations, we studied the transamination reaction for the N-protonated Schiff base. Interestingly, during the present metadynamics simulation, an intramolecular proton transfer from the N-protonated Schiff base to O-protonated Schiff base was found to occur. However, the

O-protonated state was found to be very short lived and got readily converted into the N-protonated state. Thus, the current simulations also imply that the N-protonated state of the PLP-Asp Schiff base is preferred at the active site of AspTase which corroborates with the findings of our previous study.[18]

4 | SUMMARY AND CONCLUSIONS

We have presented a QM/MM simulation study of the transamination reaction at the active site of aspartate transaminase (AspTase) enzyme. It is found that the Tyr225 residue of the enzyme exhibits two different hydrogen bonding patterns with the PLP-Asp Schiff base which suggests two possible reaction pathways for the[1,3] proton transfer process: A direct pathway from α-carbon atom of the PLP-Asp complex to the Lys258 residue of the enzyme or an indirect pathway via Tyr225. However, the reactant structure for the second pathway is found to be relatively short lived with the $Tyr_{225}O_{\eta}$...HA separation being greater than the $Lys_{258}N_{\zeta}$...HA distance. Hence, the direct pathway is considered here to study further details of the proton transfer process. The present study reveals that the transamination reaction follows a stepwise mechanism where the Lys258 residue plays the role of a catalytic base. In the first step, the Lys258 residue abstracts the α-proton of the substrate and it is then followed by the reprotonation of the PLP-Asp Schiff base through a proton transfer from Lys258 to the C4A atom of PLP. The present QM/MM simulations combined with metadynamics calculations reveal that the free energy barrier for the proton abstraction from CA atom by Lys258 is 17.85 kcal/mol and, for the reprotonation of PLP-Asp from Lys258 to C4A atom, the barrier is calculated to be 3.57 kcal/mol. The carbanionic intermediate is found to be 7.14 kcal/mol higher in energy than the external aldimine state (reactant). The Mulliken population analysis shows that the negative charge over the α-carbon atom in the intermediate state is stabilized via delocalization over the pyridine ring of PLP. The current study shows that the Lys258 undergoes a conformational change after the first step and becomes more proximal to the C4A atom. This conformational change is believed to be essential for the reprotonation of the PLP-Asp Schiff base through a proton transfer from Lys258 to the C4A atom. The active site residues Tyr70* and Gly38 anchor the Lys258 in proper position and orientation in the first step of the transamination reaction via hydrogen bonding interaction and stabilize the positive charge over the Lys258 in the intermediate state.

ACKNOWLEDGMENT

We thank Drs. Nisanth N. Nair and Ravi Tripathi for their help at the initial stage of this work. We gratefully acknowledge financial support from the Council of Scientific and Industrial Research (CSIR), and Science and Engineering Research Board (SERB), a statutory body of the Department of Science and Technology (DST), Government of India.

ORCID

Amalendu Chandra https://orcid.org/0000-0003-1223-8326

REFERENCES

[1] E. E. Snell, S. J. Di Mari, in *The Enzymes: Kinetics and Mechanism*, 3rd ed., Vol. 2 (Ed: P. D. Boyer), Academic Press, New York, NY **1970**, p. 335.
[2] P. Christen, D. E. Metzler, *Transaminases*, 1st ed., Vol. 37, Wiley, New York, NY **1985**.
[3] M. A. Spies, M. D. Toney, *Biochem.* **2003**, *42*, 5099.
[4] V. N. Malashkevich, M. D. Toney, J. N. Jansonius, *Biochem.* **1993**, *32*, 13451.
[5] J. N. Jansonius, *Curr. Opin. Struct. Biol.* **1998**, *8*, 759.
[6] J. P. Shaw, G. A. Petsko, D. Ringe, *Biochem.* **1997**, *36*, 1329.
[7] J. Jager, M. Moser, U. Sauder, J. N. Jansonius, *J. Mol. Biol.* **1994**, *239*, 285.
[8] D. L. Smith, S. C. Almo, M. D. Toney, D. Ringe, *Biochem.* **1989**, *28*, 8161.
[9] J. Thorndike, T. Pelliniemi, W. Beck, *Cancer Res.* **1979**, *39*, 3435.
[10] C. Wrenger, I. B. Muller, A. J. Schifferdecker, R. Jain, R. Jordanova, M. R. Groves, *J. Mol. Biol.* **2011**, *405*, 956.
[11] S. R. Kleppner, A. J. Tobin, *Expert Opin. Ther. Targets* **2001**, *5*, 219.
[12] C. C. Wang, *Annu. Rev. Pharmacol. Toxicol.* **1995**, *35*, 93.
[13] A. C. Eliot, J. F. Kirsch, *Annu. Rev. Biochem.* **2004**, *73*, 383.
[14] C. G. F. Stamper, A. A. Morollo, D. Ringe, *Biochemistry* **1998**, *37*, 10438.
[15] N. M. F. S. A. Cerqueira, P. A. Fernandes, M. J. Ramos, *J. Chem. Theory Comput.* **2011**, *7*, 1356.
[16] D. E. Metzler, *Biochemistry, The Chemical Reactions of Living Cells*, Academic Press, New York, NY **1977**, p. 444.
[17] K. E. Cassimjee, B. Manta, F. Himo, *Org. Biomol. Chem.* **2015**, *13*, 8453.
[18] S. Dutta Banik, A. Chandra, *J. Phys. Chem. B* **2014**, *118*, 11077.
[19] A. Okamoto, T. Higuchi, K. Hirotsu, S. Kuramitsu, H. Kagamiyama, *J. Biochem.* **1994**, *116*, 95.
[20] S. F. Velick, J. Vavra, *J. Biol. Chem.* **1962**, *237*, 2109.
[21] D. M. Kiick, P. F. Cook, *Biochem.* **1983**, *22*, 375.
[22] W. T. Jenkins, M. L. Fonda, in *Kinetics, Equilibria, and Affinity for Coenzymes and Substrates in Transaminases* (Eds: P. Christen, D. E. Metzler), Wiley and Sons, New York, NY **1985**, p. 216.
[23] K. E. Cassimjee, M. S. Humble, V. Miceli, C. G. Colomina, P. Berglund, *ACS Catal.* **2011**, *1*, 1051.
[24] D. Voet, J. G. Voet, C. W. Pratt, *Fundamentals of Biochemistry: Life at the Molecular Level*, 2nd ed., Wiley, New York, NY **2006**.
[25] R. B. Silverman, *The Organic Chemistry of Enzyme-Catalysed Reactions*, Academic Press, Elsevier Science, London **2000**.
[26] S. Rhee, M. M. Silva, C. C. Hyde, P. H. Rogers, C. M. Metzleri, D. E. Metzleri, A. J. Arnone, *Biol. Chem.* **1997**, *272*, 17293.
[27] J. F. Kirsch, G. Eichele, G. C. Ford, M. G. Vincent, J. N. Jansonius, *J. Mol. Biol.* **1984**, *174*, 497.
[28] M. M. Islam, M. Goto, I. Miyahara, H. Ikushiro, K. Hirotsu, H. Hayashi, *Biochem.* **2005**, *44*, 8218.
[29] T. Yoshimura, K.-H. Jhee, N. Esaki, K. Soda, *Bull. Inst. Chem. Res.* **1993**, *71*, 368.
[30] A. Okamoto, Y. Nakai, H. Hayashi, K. Hirotsu, H. Kagamiyama, *J. Mol. Biol.* **1998**, *280*, 443.
[31] W. Blankenfeldt, C. Nowicki, M. Montemartini-Kalisz, H. M. Kalisz, H. J. Hecht, *Protein Sci.* **1999**, *8*, 2406.
[32] R. A. Jensen, W. J. Gu, *J. Bacteriol.* **1996**, *178*, 2161.
[33] P. K. Mehta, T. I. Hale, P. Christen, *Eur. J. Biochem.* **1993**, *214*, 549.
[34] I. Miyahara, K. Hirotsu, H. Hayashi, H. Kagamiyama, *J. Biochem.* **1994**, *116*, 1001.
[35] M. D. Toney, J. F. Kirsch, *Biochem.* **1993**, *32*, 1471.

[36] H. Hayashi, H. Mizuguchi, H. Kagamiyama, *Biochem.* **1998**, *37*, 15076.
[37] Y. Park, J. Luo, P. G. Schultz, J. F. Kirsch, *Biochem.* **1997**, *36*, 10517.
[38] D. A. Julin, J. F. Kirsch, *Biochem.* **1989**, *28*, 3825.
[39] M. A. Rishavy, W. W. Cleland, *Biochem.* **2000**, *39*, 7546.
[40] B. E. C. Banks, A. A. Dianantis, C. A. Vernon, *J. Chem. Soc.* **1961**, 4235.
[41] F. V. Pishchugin, I. T. Tuleberdiev, *Russuan. J. Gen. Chem.* **2005**, *75*, 1538.
[42] R. Z. Liao, W. J. Ding, J. G. Yu, W. H. Fang, R. Z. Liu, *J. Comput. Chem.* **2008**, *29*, 1919.
[43] A. Mukherjee, R. Lavery, B. Bagchi, J. T. Hynes, *J. Am. Chem. Soc.* **2008**, *130*, 9747.
[44] A. Laio, J. VandeVondele, U. Roethlisberger, *J. Chem. Phys.* **2002**, *116*, 6941.
[45] A. Laio, J. VandeVondele, U. Roethlisberger, *J. Phys. Chem. B* **2002**, *106*, 7300.
[46] G. Jindal, A. Warshel, *J. Phys. Chem. B* **2016**, *120*, 9913.
[47] M. J. McGrath, I.-F. W. Kuo, S. Hayashi, S. Takada, *J. Am. Chem. Soc.* **2013**, *135*, 8908.
[48] S. Hayashi, Y. Uchida, T. Hasegawa, M. Higashi, T. Kosugi, M. Kamiya, *Annu. Rev. Phys. Chem.* **2017**, *68*, 135.
[49] T. Zelleke, D. Marx, *ChemPhysChem* **2017**, *18*, 208.
[50] R. Tripathi, N. N. Nair, *J. Am. Chem. Soc.* **2013**, *135*, 14679.
[51] R. Tripathi, N. N. Nair, *ACS Catal.* **2015**, *5*, 2577.
[52] H. S. Fernandes, M. J. Ramos, N. M. F. S. A. Cerqueira, *ACS Catal.* **2018**, *8*, 10096.
[53] K. Soniya, S. Awasthi, N. N. Nair, A. Chandra, *ACS Catal.* **2019**, *9*, 6276.
[54] R. Car, M. Parrinello, *Phy. Rev. Lett.* **1985**, *55*, 2471.
[55] D. A. Case, T. A. Darden, C. L. Cheatham III., T. E. Simmerling, J. Wang, R. E. Duke, R. Luo, R. C. Walker, W. Zhang, K. M. Merz, B. Wang, S. Hayik, A. Roitberg, G. Seabra, I. Kolossvai, K. F. Wong, F. Paesani, J. Vanicek, J. Liu, X. Wu, S. R. Brozell, T. Steinbrecher, H. Gohlke, Q. Cai, X. Ye, J. Wang, M. J. Hsieh, G. Cui, D. Roe, D. H. Mathews, M. G. Seetin, C. Sagui, V. Babin, T. Luchko, S. Gusarov, A. Kovalenko, P. Kollman, *AMBER 11*, University of California, San Francisco, CA **2010**.
[56] A. Laio, M. Parrinello, *Proc. Natl. Acad. Sci.* **2002**, *99*, 12562.
[57] M. Iannuzzi, A. Laio, M. Parrinello, *Phys. Rev. Lett.* **2003**, *90*, 238302.
[58] R. Graber, P. Kasper, V. N. Malashkevich, E. Sandmeier, P. Berger, H. Gehring, J. N. Jansontus, P. Christen, *Eur. J. Biochem.* **1995**, *232*, 686.
[59] J. Wang, R. M. Wolf, J. W. Caldwell, P. A. Kollman, D. A. Case, *J. Comput. Chem.* **2004**, *25*, 1157.
[60] Version III.3. RED: RESP ESP charge Derive. See also http://q4md-forcefieldtools.org/RED/.
[61] W. L. Jorgensen, J. Chandrasekhar, J. D. Madura, R. W. Impey, M. L. Klein, *J. Chem. Phys.* **1983**, *79*, 926.
[62] J. Hutter, A. Alavi, T. Deutsch, M. Bernasconi, S. Goedecker, D. Marx, M. E. Tuckerman, M. Parrinello, *CPMD Program Package*, IBM Corp. and Max Planck Institute, Stuttgart **2000** See also http://www.cpmd.org.
[63] A. D. Becke, *Phys. Rev. A* **1988**, *38*, 3098.
[64] C. Lee, W. Yang, R. G. Parr, *Phys. Rev. B* **1988**, *37*, 785.
[65] N. Troullier, J. L. Martins, *Phys. Rev. B* **1991**, *43*, 1993.
[66] A. Barducci, M. Bonomi, M. Parrinello, *Adv. Rev.* **2011**, *1*, 826.
[67] A. Laio, F. L. Gervasio, *Rep. Prog. Phys.* **2008**, *71*, 126601.
[68] O. Valsson, P. Tiwary, M. Parrinello, *Annu. Rev. Phys. Chem.* **2016**, *67*, 159.
[69] M. Boero, T. Ikeshoji, C. C. Liew, K. Terakura, M. Parrinello, *J. Am. Chem. Soc.* **2004**, *126*, 6280.
[70] M. Alfonso-Prieto, H. Oberhofer, M. L. Klein, C. Rovira, J. Blumberger, *J. Am. Chem. Soc.* **2011**, *133*, 4285.
[71] H. Schlegel, P. E. Zaoralek, P. Christen, *J. Biol. Chem.* **1977**, *252*, 5835.
[72] S. E. Wilkie, M. Warren, J. Protein, *Exp. Purif.* **1998**, *12*, 381.
[73] M. Campos-Cavieres, E. A. Munn, *Biochem. J.* **1973**, *135*, 683.
[74] Y. Nobe, S. Kawaguchi, H. Ura, T. Nakai, K. Hirotsu, R. Kato, S. Kuramitsu, *J. Biol. Chem.* **1998**, *273*, 29554.
[75] N. Nandi, *Chirality in biological Nanospace: Reactions in Active Sites*, CRC Press Taylor and Francis, Boca Raton **2011**.
[76] Y. L. Lin, J. Gao, *J. Am. Chem. Soc.* **2011**, *133*, 4398.
[77] Y. L. Lin, J. Gao, *Biochem.* **2010**, *49*, 84.
[78] W. Humphrey, A. Dalke, K. Schulten, *J. Mol. Graphics* **1996**, *14*, 33.

How to cite this article: Dutta Banik S, Bankura A, Chandra A. A QM/MM simulation study of transamination reaction at the active site of aspartate aminotransferase: Free energy landscape and proton transfer pathways. *J Comput Chem.* 2020;1–11. https://doi.org/10.1002/jcc.26422